Mapping of a many-qubit state onto an oscillator using controlled displacements

Bjerrum, Anders J. E.; Andersen, Ulrik L.; Rabl, Peter

Published in:
Physical Review A

Link to article, DOI:
10.1103/fdx5-kftm

Publication date:
2025

Document Version
Publisher's PDF, also known as Version of record

Citation (APA):
Bjerrum, A. J. E., Andersen, U. L., & Rabl, P. (2025). Mapping of a many-qubit state onto an oscillator using controlled displacements. *Physical Review A*, *111*(6), Article 062613. https://doi.org/10.1103/fdx5-kftm

Mapping of a many-qubit state onto an oscillator using controlled displacements

Anders J. E. Bjerrum and Ulrik L. Andersen
Center for Macroscopic Quantum States (bigQ), Department of Physics, Technical University of Denmark, 2800 Kongens Lyngby, Denmark

Peter Rabl
Walther-Meißner-Institut, Bayerische Akademie der Wissenschaften, 85748 Garching, Germany; Technische Universität München, TUM School of Natural Sciences, Physics Department, 85748 Garching, Germany; and Munich Center for Quantum Science and Technology (MCQST), 80799 Munich, Germany

(Received 24 October 2024; accepted 24 April 2025; published 11 June 2025)

We extend the controlled displacement interaction between a qubit and a harmonic oscillator to the multiqubit (qudit) case. We define discrete quadratures of the qudit and show how the qudit state can be displaced in these quadratures controlled by an oscillator quadrature. Using this interaction, a periodic repetition of the state encoded in the qudit, can be deterministically mapped onto the oscillator, which is initialized in a squeezed state. Based on this controlled displacement interaction, we present a full circuit that encodes quantum information in a superposition of qudit quadrature states, and successively prepares the oscillator in the corresponding superposition of approximate Gottesman-Kitaev-Preskill (GKP) states. This preparation scheme is found to be similar to phase estimation, with the addition of a disentanglement gate. Our protocol for GKP state preparation is efficient in the sense, that the set of qubits need only interact with the oscillator through two time-independent interactions, and in the sense that the squeeze factor (in dB) of the produced GKP state grows linearly in the number of qubits used.

DOI: 10.1103/fdx5-kftm

I. INTRODUCTION

We present a protocol for deterministically mapping a state encoded in a set of qubits onto an oscillator. This mapping is utilized to generate approximate Gottesman-Kitaev-Preskill (GKP) states [1], which have been given much attention in the literature as a promising candidate for encoding an error correctable qubit in an oscillator [2,3]. These states can be protected against small shifts in phase space, and will be relevant to implementations of bosonic quantum computing [4,5] and also quantum communication [6–9].

Various methods for preparing GKP states exist in the literature including Floquet engineering [10], cavity QED [11,12], cat breeding [13,14], boson sampling [15,16], phase estimation [17,18], the dispersive Faraday interaction [19], and shaped free electrons [20]. We note that experimental realizations of approximate GKP states have been achieved in trapped ion systems [21,22], and superconducting microwave cavities [23,24]. In this work we present a protocol for preparing GKP states, which utilize a many-qubit state. By leveraging the rich structure of multiple qubits, we show that by tailoring the qudit state we can efficiently prepare approximate GKP states of the oscillator. Efficient in the sense that the squeeze factor (in dB) of the GKP state grows linearly in the number of employed qubits, and in the sense that the set of qubits need only interact with the oscillator through two time-independent interactions. Our scheme is highly related to phase estimation, however, our protocol does not require any measurements to be performed. We expect that the scheme proposed in this work could be implemented using superconducting microwave cavities as in [24], but also in other platforms.

The noncommutativity between the q and p quadrature operators, as dictated by the canonical commutation relation of quantum optics $[q, p] = i$ (setting the vacuum variance to 1/2) enforces that no common eigenstates exist for q and p. However, the corresponding modular observables $q_m = q \pmod{Q}$ and $p_m = p \pmod{\frac{2\pi}{Q}}$ posses common eigenstates [1,25] for any real number Q, and these states can be written as,

$$|q_0, p_0\rangle = \sum_{s=-\infty}^{\infty} e^{ip_0(q_0-sQ)}|q_0 - sQ\rangle, \tag{1}$$

with q_0 and p_0 being the eigenvalues of q_m and p_m, respectively. We note that $|q_0, p_0\rangle$ is not normalizable, and does not constitute a proper quantum state. However, these states can be closely approximated, with GKP states providing a practical representation. The GKP states can be expressed as,

$$|G(\phi)\rangle = \mathcal{N}_0 \sum_{s=-\infty}^{\infty} e^{-(\kappa(2s+\phi)\sqrt{\pi})^2/2} \int_{-\infty}^{\infty} dq \pi^{-1/4}\Delta^{-1/2} \times e^{-q^2/(2\Delta^2)} |q + (2s+\phi)\sqrt{\pi}\rangle, \tag{2}$$

where $\mathcal{N}_0$ is the normalization. In position space, these states represent a train of peaks of width Δ and spacing $2\sqrt{\pi}$. The parameter κ determines the overall gaussian envelop, and ϕ shifts the center of the GKP state. By choosing $\phi = 0$ and

$\phi = 1$ we obtain two orthogonal states (for small enough Δ), which can be identified with the logical qubit states $|0_L\rangle \equiv |G(0)\rangle$ and $|1_L\rangle \equiv |G(1)\rangle$, respectively.

Starting from of an oscillator prepared in a squeezed vacuum state, the central task is to prepare the oscillator in a superposition of displaced gaussian wave packets, which represents an arbitrary qubit state $|\psi_L\rangle = \alpha|0_L\rangle + \beta|1_L\rangle$. Previous works have demonstrated [11,17,24,26] that the preparation of GKP states can be achieved using controlled displacement interactions between a qubit and an oscillator. Controlled displacements allow us to displace the oscillator in the p quadrature, conditional on the spin state of the qubit, and are generated by the Hamiltonian,

$$H_{\text{int}}/\hbar = \chi q \sigma_z, \tag{3}$$

where σ_z is the Pauli z operator for the qubit, and χ is a coupling frequency. We have the σ_z eigenstates $\sigma_z|0\rangle = |0\rangle$ and $\sigma_z|1\rangle = -|1\rangle$. This approach requires a repeated interaction between qubit and oscillator, and after each step the qubit must be disentangled from the resonator either via a projective measurement or a disentangling gate. Imperfections in these operations as well as the decoherence of the qubit during the interaction limit the achievable fidelity of the prepared state [24].

In the following we present a different preparation strategy where the sequential interaction with a single qubit is replaced by a single parallel interaction with $N > 1$ qubits. To do so we consider a qubit-oscillator coupling of the form

$$H_{\text{int}}/\hbar = \chi q X_N, \tag{4}$$

where $X_N = -\sum_{n=1}^{N} 2^{n-2}\sigma_z^{(n)}$ is the discrete quadrature operator in the N-qubit subspace. We are not aware of any existing experimental demonstration of such an interaction. A difficulty associated with this interaction is that multiple qubits would have to couple to the same oscillator with varying coupling rates. By preparing an appropriate initial state of the qubits, this interaction allows us to prepare an arbitrary encoded state $|\psi_L\rangle$ by a single global controlled displacement gate and one global disentangling operation. In this way, the interaction time, during which the state is sensitive to qubit dephasing, is minimized and most of the gates for preparing the required initial qubit state can be implemented while the oscillator and the qubits are decoupled.

Given an initial oscillator state with q-quadrature wave function $\psi(q) = \langle q|\psi\rangle \propto \exp(-\frac{q^2}{2W^2})$ of width $W > 1$ (antisqueezed in q), our protocol will produce GKP states with an envelope,

$$\kappa = \frac{1}{W}, \tag{5}$$

while the width of the individual peaks decreases exponentially with the number of qubits,

$$\Delta \propto 2^{-N}, \tag{6}$$

with a proportionality constant of around 3.1. For $N = 3$ and $N = 4$ qubits, we find that the protocol ideally produces approximate GKP states with $\Delta \approx 0.39$ (8.2 dB) and $\Delta \approx 0.19$ (14.4 dB), respectively.

Qudit quadratures

Before we describe the actual protocol, we start by outlining the underlying theory. We define discrete quadrature operators for a qudit [27,28]. We then realize the qudit using a set of qubits, and the qudit quadratures are then constructed from the Hamiltonian of this system. Finally, we present a unitary that displaces the qudit in one of the qudit quadratures, conditioned on an oscillator quadrature.

Given a qudit of dimension M, we denote the qudit levels by the basis states $|x_k\rangle$ where k is a number belonging to the set,

$$k \in K = \{\pm 1/2, \pm 3/2, \cdots, \pm (M-1)/2\}. \tag{7}$$

The basis states $|x_k\rangle$ can for example be realized as the logical basis states of a set of qubits, as we will show in the next section. Using these states we introduce a discrete operator,

$$X_N = \sum_{k\in K} k\, |x_k\rangle\langle x_k|\,. \tag{8}$$

We refer to X_N as a quadrature operator because it has a linear spectrum with both positive and negative values. Applying the discrete Fourier transform, i.e., the quantum Fourier transform F_N, we can transform X_N into a conjugate quadrature operator,

$$Y_N = F_N X_N F_N^{\dagger}, \tag{9}$$

where

$$F_N = \frac{1}{\sqrt{M}} \sum_{n,m\in K} e^{i2\pi(n-1/2)(m-1/2)/M}\, |x_m\rangle\langle x_n|, \tag{10}$$

and Y_N has eigenvectors,

$$|y_n\rangle = \frac{1}{\sqrt{M}} \sum_{k\in K} e^{i2\pi(n-1/2)(k-1/2)/M}\, |x_k\rangle, \tag{11}$$

with eigenvalues $n \in K$.

We will now argue that Y_N is the generator of translations in the qudit levels. To see this we introduce the qudit state $|v\rangle$ with amplitudes v_k,

$$|v\rangle = \sum_{k\in K} v_k\, |x_k\rangle, \tag{12}$$

and note that the following expression interpolates the points (k, v_k) over the interval $y \in R_0 = [-M/2, M/2[$,

$$v(y) = \frac{1}{M} \sum_{n,l\in K} v_l e^{i2\pi(n-1/2)(y-l)/M}, \tag{13}$$

as can be verified by evaluating $v(k)$ for $k \in K$. Extending the range of y outside R_0 shows that $v(y)$ repeats itself with period M. More details on $v(y)$ can be found in Appendix 1.

We then exponentiate Y_N as $D_x(s) = e^{-i\frac{2\pi}{M}Y_N s}$ where s is an arbitrary real number. Evaluating the action of $D_x(s)$ on the state $|v\rangle$, we obtain,

$$D_x(s) \sum_{k\in K} v_k |x_k\rangle = e^{-i\frac{\pi}{M}s} \sum_{m\in K} v(m-s)|x_m\rangle. \tag{14}$$

Hence the action of $D_x(s)$ on $|v\rangle$ is to generate a new qudit state, where the amplitudes of this new state are obtained by sampling from a translation of the interpolating function $v(y)$.

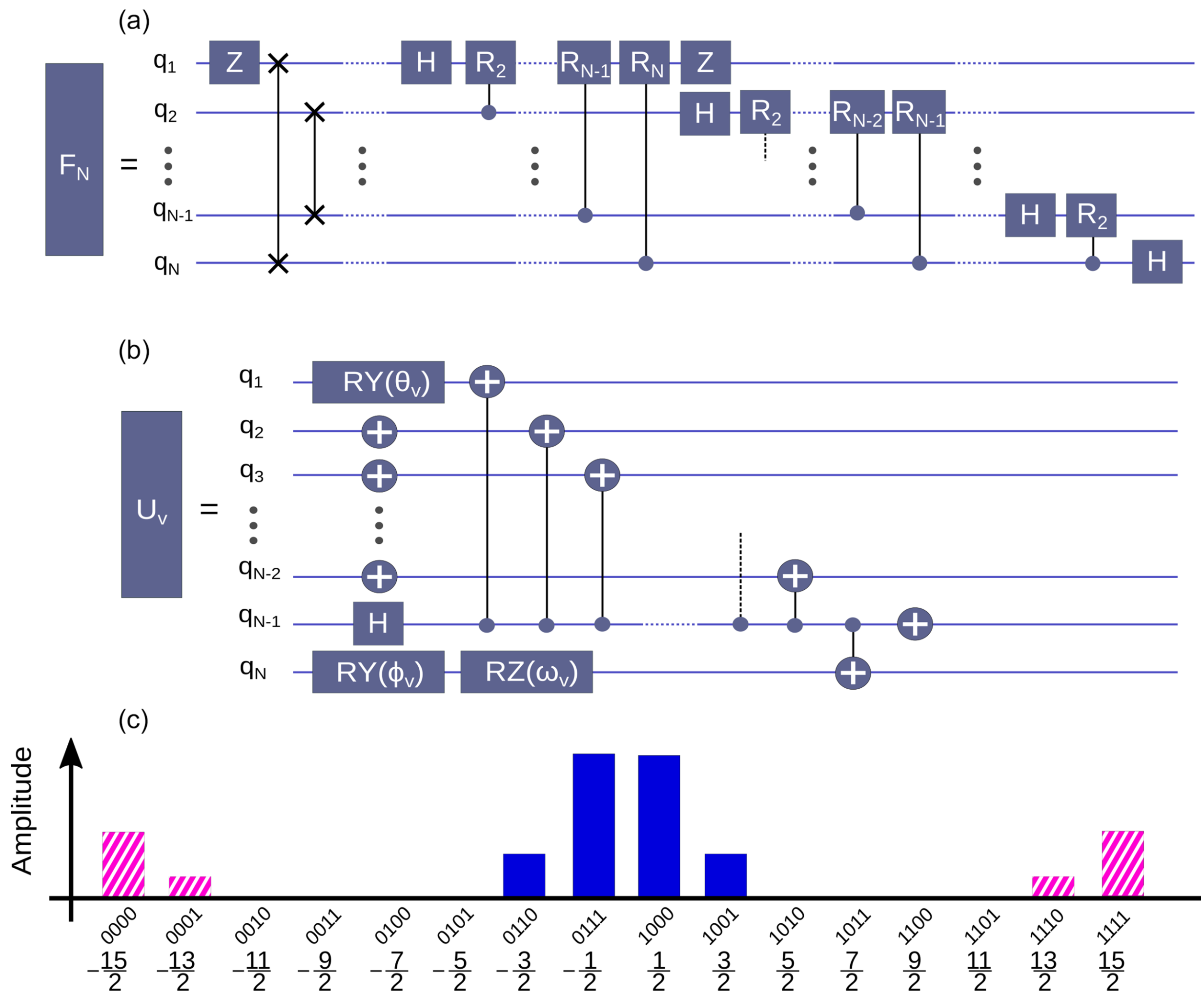

FIG. 1. (a) Quantum circuit for the version of the quantum Fourier transform used in this work. The connected crosses indicate a swap gate. (b) Circuit for preparing the family of qubit states $|v\rangle$. The circuit corresponds to the unitary U_v. The encircled plus symbol is a Pauli x gate. The controlled gates are controlled not gates, and the target qubit is denoted by an encircled plus. θ_v is chosen so that the resulting state resembles a Gaussian distribution, we find that $\theta_v = 2.6$ works well. This distribution can be brought into an arbitrary superposition of two central positions by tuning the relative amplitude via ϕ_v and the relative phase via ω_v. (c) A sketch of a quantum state generated by the unitary U_v given in (b), with four qubits initially in the state $|0, 0, 0, 0\rangle$, and with $\theta_v = 2.6$. On the x axis we give the logical state of the qubits, and the associated eigenvalue of the X_N operator. On the y axis we sketch the amplitudes, with color and texture indicating phase. If we impose periodic boundary conditions, we note that the state is a superposition of two localized peaks. The relative amplitude and phase of these peaks are controlled by ϕ_v and ω_v, respectively.

Qubit realization

Given a collection of N qubits we form a qudit of dimension $M = 2^N$. The qudit levels are now the associated logical basis states, $|x_k\rangle = |j_N, j_{N-1}, \ldots, j_2, j_1\rangle$, where $j_n \in \{0, 1\}$. The label k is related to the logical state as,

$$k = \sum_{n=1}^{N} j_n 2^{n-1} - (M-1)/2. \tag{15}$$

The circuit for generating the QFT F_N is shown in Fig. 1(a) [27]. This circuit uses the gate R_k which can be written in the σ_z basis ($|0\rangle = (1 \quad 0)^T$) as

$$R_k = \begin{pmatrix} 1 & 0 \\ 0 & e^{2\pi i/2^k} \end{pmatrix}. \tag{16}$$

We construct the quadrature operator X_N using the $\sigma_z^{(n)}$ operators,

$$X_N = -\sum_{n=1}^{N} 2^{n-2}\sigma_z^{(n)}, \tag{17}$$

where $\sigma_z^{(n)}$ is applied to the n-th qubit. Assuming we have access to a controlled displacement between each of the qubits and an oscillator, we assume a qubit-oscillator coupling of the form

$$H_{\text{int}}/\hbar = \chi q X_N = -\chi \sum_{n=1}^{N} 2^{n-2} q\sigma_z^{(n)}, \tag{18}$$

where q is a quadrature of the oscillator. Applying the QFT and evolving under the time-independent Hamiltonian $H_{\text{int}}/\hbar$

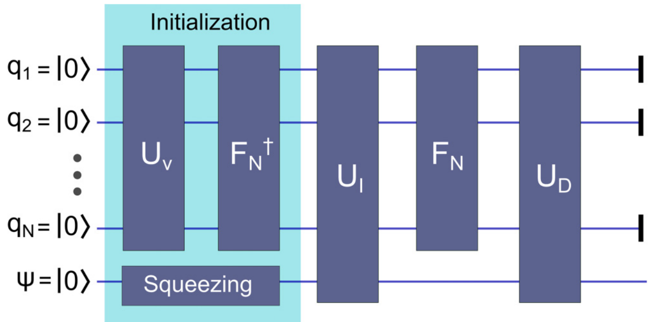

FIG. 2. Sketch of the protocol given in the main text. The circuit U_v generates the initial qubit state. We apply the inverse QFT on the qubits, and we then apply the unitary U_I. The QFT is then applied on the qubits, and a disentangling operation U_D follows.

for a time τ_I, we observe the following result,

$$F_N e^{i\chi\tau_I q X_N} F_N^\dagger = e^{i\chi\tau_I q Y_N} = D_x\left(-\frac{Mq}{P_q}\right), \tag{19}$$

where we have defined the dimensionless parameter $P_q = 2\pi/(\chi\tau_I)$. Hence if we have access to controlled displacements and the QFT, then we can displace the qubit state through the X_N quadrature, conditioned on the quadrature q of an oscillator.

II. PROTOCOL

We can now describe our protocol, which is sketched in Fig. 2. The protocol proceeds as follows,

(1) The initial oscillator state $\psi_0(q)$ is a displaced squeezed state in the q quadrature, $\psi_0(q) = e^{-iq\pi/P_q}\psi_W(q)$, where $\psi_W(q) = C\exp(-\frac{q^2}{2W^2})$ is squeezed vacuum of width $W > 1$, i.e., we have antisqueezin

(2) The qubits are initialized in the state $|v\rangle = U_v|0, 0, 0, \ldots, 0\rangle$.

(3) The inverse QFT is applied to the qubits.

(4) The qubits interact with the oscillator through the unitary $U_I = e^{i(2\pi/P_q)qX_N}$.

(5) The QFT is applied to the qubits.

(6) The qubits interact with the oscillator through $U_D = e^{-i(P_q/M)pX_N}$.

To implement our protocol we prepare the qubit state $|v\rangle$ using the circuit shown in Fig. 1(b), which acts on the input state $|0, 0, \ldots, 0\rangle$. A sketch of the amplitudes associated with the state $|v\rangle$ is shown in Fig. 1(c). The final result of our protocol is to map the interpolation $v(y)$ of the state $|v\rangle$ onto the oscillator in a periodic fashion. The state $|v\rangle$ is therefore chosen such that its periodic continuation yields a train of peaks. In particular we aim for $v(y)$ to produce two sets of peaks: one set that is associated with the logical 0 GKP state, and one set that is associated with the logical 1 GKP state. The circuit shown in Fig. 1(b) is denoted by the unitary U_v, so we may write $|v\rangle = U_v|0, 0, \ldots, 0\rangle$. We have defined the operators $\mathrm{RY}(\phi_v) = e^{-i(\phi_v/2)\sigma_y}$ and $\mathrm{RZ}(\omega_v) = e^{-i(\omega_v/2)\sigma_z}$. The angles ϕ_v and ω_v are used to create an arbitrary superposition of two central positions, as shown in Fig. 1(c), with ϕ_v controlling the relative amplitude and ω_v controlling the relative phase, such that the protocol prepares the GKP state $|\Psi_L\rangle = \cos(\phi_v/2)|0_L\rangle + \sin(\phi_v/2)e^{i\omega_v}|1_L\rangle$. We set $\theta_v = 2.6$ as this generates a qubit state with approximately Gaussian peaks, as sketched in Fig. 1(c). For θ_v outside the range [2.5,2.7] the function $v(y)$, which interpolates the qubit state, will have a significant amount of undesirable oscillations. Breaking down the protocol, we examine the following term,

$$\begin{aligned} F_N U_I F_N^\dagger |v\rangle|\psi_0\rangle &= \int_{-\infty}^{\infty} dq D_x\left(-\frac{M}{P_q}q\right)|v\rangle\,\psi_0(q)\,|q\rangle \\ &= \sum_{l\in K}\int_{-\infty}^{\infty} dq v\left(l+\frac{M}{P_q}q\right)\psi_W(q)\,|x_l\rangle\,|q\rangle, \end{aligned} \tag{20}$$

showing that the interaction has the effect of modulating the squeezed vacuum $\psi_W(q)$ by the periodic function $v(l+\frac{M}{P_q}q)$ with period P_q in q.

Next, we apply the unitary U_D on the qubits and the oscillator, and we will see that U_D approximately disentangles the qubits and oscillator. Applying U_D we get,

$$\begin{aligned} &U_D F_N U_I F_N^\dagger |v\rangle|\psi_0\rangle \\ &= \int_{-\infty}^{\infty} dq\psi_W(q)\sum_{l\in K} v\left(l+\frac{M}{P_q}q\right)e^{-i\frac{P_q}{M}pX_N}\,|x_l\rangle\,|q\rangle \\ &= \int_{-\infty}^{\infty} dq\psi_W(q)\sum_{l\in K} v\left(l+\frac{M}{P_q}q\right)|x_l\rangle\left|q+l\frac{P_q}{M}\right\rangle \\ &= \int_{-\infty}^{\infty} dq\sum_{l\in K}\psi_W\left(q-l\frac{P_q}{M}\right)v\left(\frac{M}{P_q}q\right)|x_l\rangle\,|q\rangle. \end{aligned} \tag{21}$$

Provided that $\psi_W(q)$ varies slowly in q, so that it does not change significantly over the period P_q, then we observe that there is only a small amount of entanglement between the oscillator and the qubits in the above expression, since l is bounded by $\pm M/2$. This condition holds approximately if $W > P_q/2$. Under this assumption we can rewrite Eq. (21) as,

$$U_D F_N U_I F_N^\dagger |v\rangle|\psi_0\rangle \approx \int_{-\infty}^{\infty} dq\psi_W(q)v\left(\frac{M}{P_q}q\right)|q\rangle\sum_{l\in K}|x_l\rangle, \tag{22}$$

showing that the oscillator state is now antisqueezed vacuum modulated by the periodic function $v(\frac{M}{P_q}q)$. The antisqueezed vacuum $\psi_W(q)$ corresponds to the envelope in Eq. (2), whereas the width of $v(\frac{M}{P_q}q)$ in q corresponds to Δ in Eq. (2). The standard deviation of $v(y)$ is $\sigma = 0.83$ for $\theta_v = 2.6$. Since $M = 2^N$ we find that the width of $v(\frac{M}{P_q}q)$ in q, and hence Δ, scales as,

$$\Delta \approx \frac{\sigma P_q}{2^N}, \tag{23}$$

where $\sigma P_q \approx 2.9$. However, $v(y)$ is not perfectly Gaussian, and by numerically fitting the expression in Eq. (2) to the states generated by the protocol, we find better agreement with the relation $\Delta \approx 3.1/2^N$. It follows that the squeeze factor (in dB) of the approximate GKP state will grow linearly in the number of qubits N.

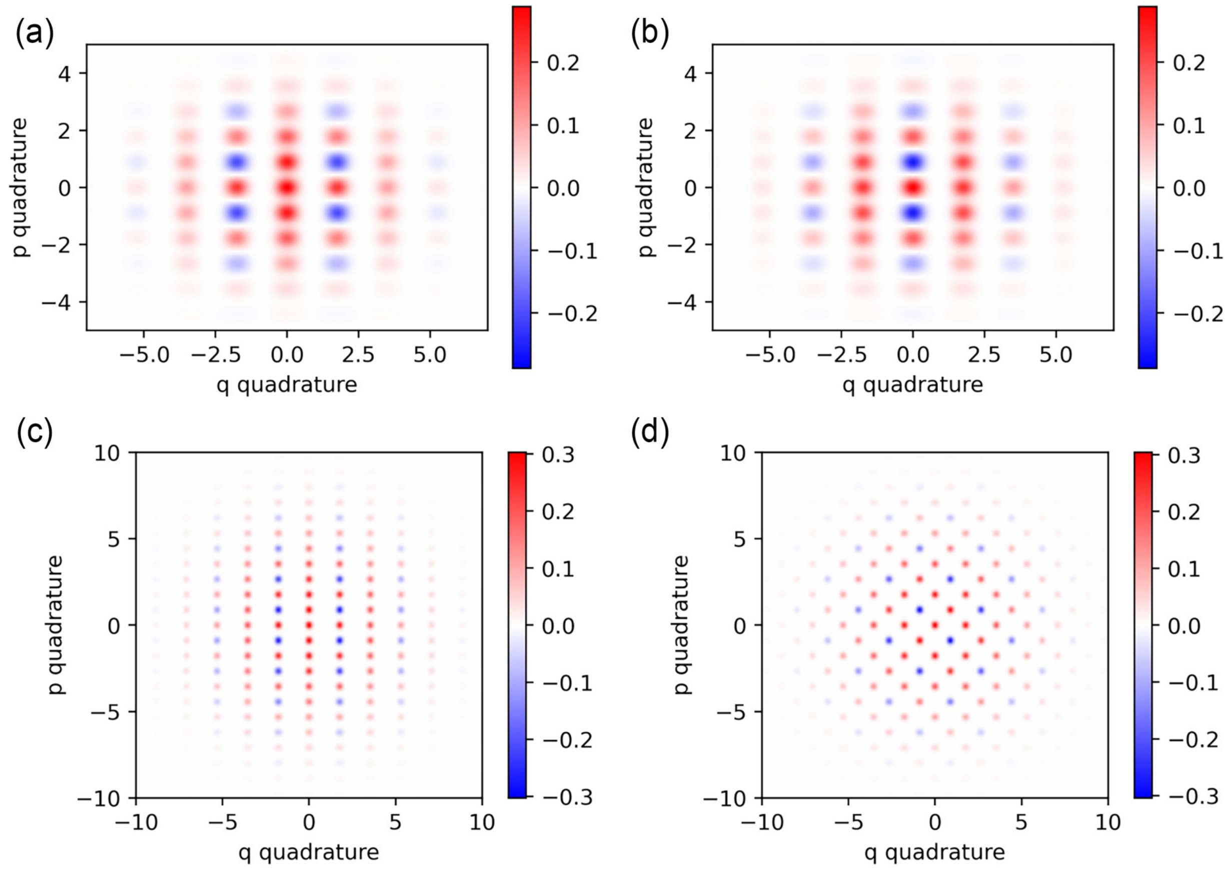

FIG. 3. Wigner functions for states created by the protocol. (a) Wigner function for three qubits with 10 dB of initial squeezing, i.e., $W = 3.2$. Furthermore we have $\phi_v = \omega_v = 0$ and $P_q = 2\sqrt{\pi}$. The Wigner function is seen to strongly resemble a logical 0 GKP state. (b) Wigner function for 3 qubits with 10 dB of initial squeezing, $\phi_v = \pi$ and $\omega_v = 0$. The Wigner function is seen to strongly resemble a logical 1 GKP state. (c) Wigner function for four qubits with 14 dB of initial squeezing and $\phi_v = \omega_v = 0$. (d) Wigner function for four qubits with 14 dB of initial squeezing and $\phi_v = \pi/2$ and $\omega_v = \pi/2$.

Without invoking the above approximation we can describe the state of the oscillator using the reduced density matrix,

$$\rho_\psi = \int_{-\infty}^{\infty} dz \int_{-\infty}^{\infty} dy \sum_{l\in K} \psi_W\left(z - l\frac{P_q}{M}\right)\psi_W\left(y - l\frac{P_q}{M}\right)^* \times v\left(\frac{M}{P_q}z\right)v\left(\frac{M}{P_q}y\right)^* |z\rangle\langle y| . \tag{24}$$

We plot the Wigner function of the state in Eq. (24) for various values of N and W, using $\theta_v = 2.6$. The results are shown in Fig. 3.

Implementation with a dispersive Hamiltonian

Following the approach in Ref. [24] we show how to implement the controlled displacements used in our protocol. This approach leverages a dispersive interaction between the qubits and the oscillator. In the dispersive regime, we assume the following Hamiltonian [29],

$$H/\hbar = \sum_{n=1}^{N}\left\{\chi^{(n)} a^\dagger a \frac{\sigma_z^{(n)}}{2} + \frac{1}{2}\omega_q^{(n)}\sigma_z^{(n)}\right\} + \varepsilon^*(t)a + \varepsilon(t)a^\dagger + \omega_o a^\dagger a, \tag{25}$$

where the drive $\varepsilon(t)$ is resonant with the oscillator. ω_o and $\omega_q^{(n)}$ are oscillator and qubit frequencies respectively. This drive will perform displacements in phase space to engineer the target controlled displacement gate between the qubits and the oscillator. We assume that the coupling frequencies can be arranged such that $\chi^{(n)} = \chi 2^{n-2}$. Considering a transmon-oscillator dispersive interaction, one finds that the coupling frequency $\chi^{(n)}$, can for example be varied by changing the detuning or charging energy of the transmon [29]. We also note the exponential scaling of the coupling frequencies $\chi^{(n)}$, a feature shared with the related standard phase estimation protocol [17], but which the authors circumvent by replacing standard phase estimation with phase estimation by repetition. It is crucial that the relative error on these coupling frequencies is small, ensuring that the error on the largest coupling frequency is small compared to the magnitude of the smallest coupling frequency. This required exponential scale of coupling frequencies $\chi^{(n)}$, implies that our protocol has a significant sensitivity toward the relative error on the coupling frequencies $\chi^{(n)}$.

The density matrix ρ of the joint qubits-oscillator system evolves according to a master equation, given in Lindblad form as,

$$\partial_t \rho = -i[H/\hbar, \rho] + \sum_i \kappa_i D[L_i]\rho \tag{26}$$

TABLE I. Table of noise sources and their associated jump operator and rate [24,30].

Jump operator L_i	Rate κ_i	Description
a	κ_l	Photon loss
$\sigma_-^{(n)}$	γ_l	Qubit decay
$a^\dagger a$	$2\kappa_\phi$	Oscillator phase noise
$\frac{1}{2}\sigma_z^{(n)}$	$2\gamma_\phi$	Qubit phase noise

with $D[L_i]$ being the Lindbladian associated with operator L_i,

$$D[L_i] = L_i\rho L_i^\dagger - \tfrac{1}{2}(L_i^\dagger L_i\rho + \rho L_i^\dagger L_i), \tag{27}$$

and κ_i is the associated rate. We include in our analysis the noise sources listed in Table I. Following Ref. [24], we transition to a displaced rotated frame $\mathcal{D}$, as detailed in the Appendix Secs. 2–5. In this displaced frame we shift the origin in phase space such that the ordinary vacuum state is a displaced coherent state. It is useful to work in a displaced frame when simulating states that are localized and centered far out in phase space. While such states will have a high photon number in the ordinary frame, they might have a low photon number in the displaced frame. We introduce the complex number $\alpha(t)$ such that $|-\alpha(t)\rangle\langle-\alpha(t)|$ represents the vacuum state in the ordinary frame as viewed from the displaced frame $\mathcal{D}$. In frame $\mathcal{D}$ we have the effective Hamiltonian,

$$H_{\text{eff}}/\hbar = \sum_{n=1}^{N}\left\{\frac{1}{2}\chi^{(n)}a^\dagger a\sigma_z^{(n)} + \frac{1}{2}\chi^{(n)}|\alpha(t)|^2\sigma_z^{(n)} + \frac{1}{2}\chi^{(n)}(\alpha(t)a^\dagger + \alpha^*(t)a)\sigma_z^{(n)}\right\}, \tag{28}$$

where the drive $\varepsilon(t)$ satisfies,

$$e^{i\omega_o t}\varepsilon(t) - i\dot{\alpha}(t) - \tfrac{1}{2}i\kappa_l\alpha(t) = 0. \tag{29}$$

It was demonstrated in Ref. [24] that the term $\frac{1}{2}\sum_{n=1}^{N}\chi^{(n)}a^\dagger a\sigma_z^{(n)}$ can be suppressed by flipping the qubits and $\alpha(t)$ after half of the interaction time. By suppressing this term the effective Hamiltonian H_{eff} becomes the desired controlled displacement interaction. We will assume that the qubit rotation $\frac{1}{2}\chi^{(n)}|\alpha(t)|^2\sigma_z^{(n)}$ can be corrected for and it is ignored in the following analysis.

III. DISCUSSION

The idealized time-dependent displacement $\alpha(t)$ that implements our protocol is sketched in Fig. 4. The figure also shows the timing for qubit flips and the application of the QFT. Note that in an experimental implementation the idealized sharp steps of $\alpha(t)$ will be replaced by a smoothly varying function resulting from a realistic drive $\varepsilon(t)$ [24]. The interaction time between the qubits and the oscillator is divided into τ_I and τ_D, corresponding to the implementation of U_I and U_D, respectively. These intervals are given by,

$$\tau_I = \frac{2\sqrt{2}\pi}{\alpha_0\chi P_q}$$
$$\tau_D = \frac{\sqrt{2}P_q}{\alpha_0\chi M}, \tag{30}$$

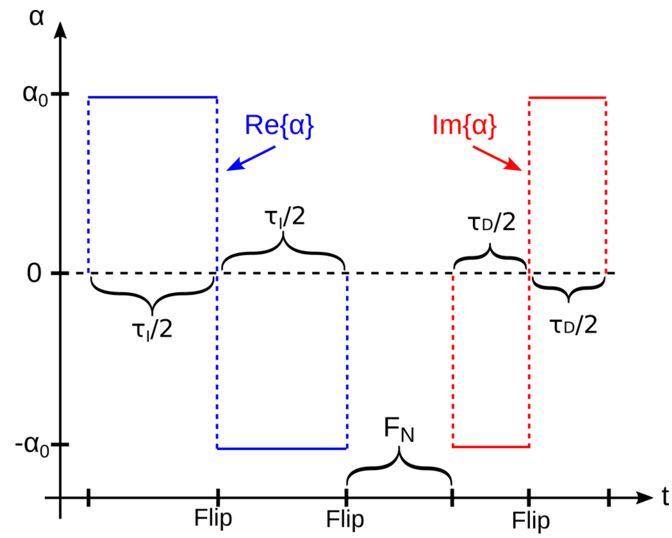

FIG. 4. Ideal time dependence of $\alpha(t)$ that implements our protocol, with three qubit flips. The resulting state for $P_q = 2\sqrt{\pi}$ can be seen in Fig. 5. On the time axis we show the operations applied only to the qubits, where F_N is the QFT.

where $\alpha_0 = \max(|\alpha(t)|)$ is the maximum displacement amplitude. The peak spacing P_q is set to $2\sqrt{\pi}$.

From now on we set χ to 1, since in the absence of decoherence, χ is the only rate in our equation of motion. The noise rates, given in Table I, are initially set to zero, but will later be defined relative to $\chi_{\max} = 2^{N-2}\chi$. In Fig. 5 we plot the Wigner function of the state resulting from the drive $\alpha(t)$ (Fig. 4) with three qubits and an initial squeezing of 10 dB. Instead of doing three qubit flips as in Fig. 4, the qubits are instead flipped seven times. This reduces a distortion of the state resulting from the terms $a^\dagger a\sigma_z^{(n)}$. The produced state closely matches the target state shown in Fig. 3(a), with a slight slant that diminishes if the qubits are flipped more often during the protocol, or if α_0 is increased.

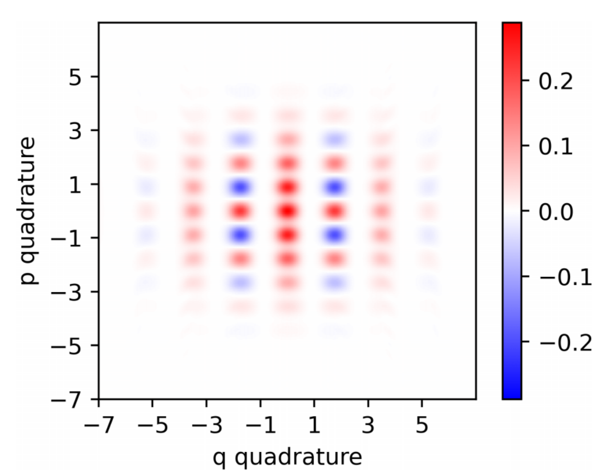

FIG. 5. Wigner function of the oscillator state resulting from the sequence given in Fig. 4 with three qubits. We have set $\chi = 1$, $P_q = 2\sqrt{\pi}$, and $\alpha_0 = 30$ (as in Ref. [24]). The qubits are flipped seven times. The slight slant is due to the interaction terms $a^\dagger a\sigma_z^{(n)}$ and vanishes if the qubits are flipped for more often, or α_0 is increased.

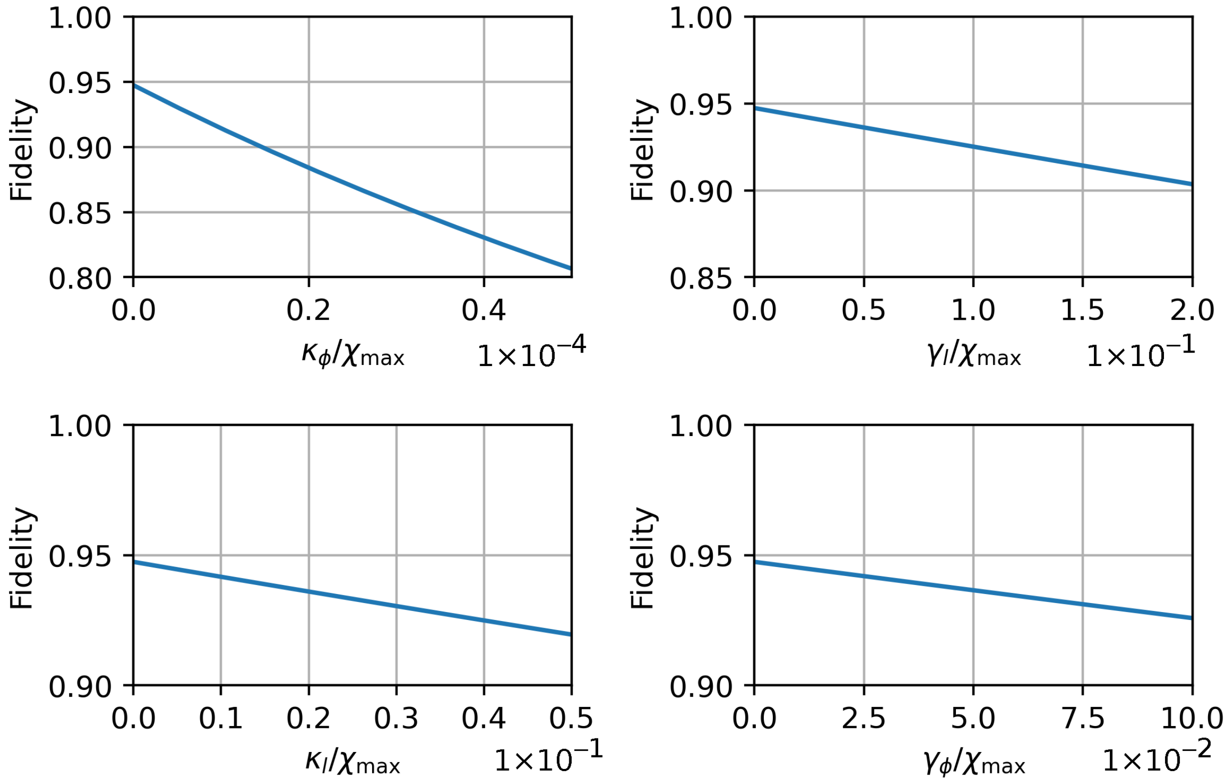

FIG. 6. Fidelity between G_0 and ρ_κ for various noise rates (see main text). On the x axis we give the ratio between the noise rate and $\chi_{\max}$. χ is set to 1 and defines the time-scale of the simulation. α_0 is set to 30. The plots do not include decoherence effects associated with the implementation of the QFT.

We evaluate the robustness of the protocol to dephasing and loss during the controlled displacement sequence. Robustness is measured in terms of the fidelity between the produced state and the target GKP state. Assuming the protocol produces the state ρ_0 in the absence of noise, we determine the approximate GKP state G_0 [as given in Eq. (2)] most similar to ρ_0, as measured by the fidelity. The state produced in the presence of noise with rate κ, is denoted ρ_κ. To gauge the sensitivity of the scheme to the noise sources listed in Table I, we compute the fidelity between ρ_κ and G_0 as we vary the noise rates individually. Plots of the fidelity against the noise rates are given in Fig. 6. The noise rates are chosen so as to be comparable with the rates given in Ref. [24]. We set $\alpha_0 = 30$ (as in Ref. [24]). The calculations do not include decoherence effects associated with the initialization of the qubits and oscillator (see Fig. 2), and the implementation of the QFT. We expect that the error channels associated with these operations might make our protocol more error prone than the comparable protocols [17] and [24].

The protocol appears stable against oscillator loss and qubit noise. The controlled displacement is, however, sensitive to oscillator phase noise, due to the large displacement α_0. The nonunit fidelity at zero noise results from the peaks not being perfect Gaussians, finite squeezing of the initial wave function, and from a distortion generated by the $a^\dagger a\sigma_z^{(n)}$ interaction.

IV. CONCLUSIONS

We have presented a protocol for mapping a qudit state onto an oscillator using the periodic interpolating function $v(y)$ defined in Eq. (13). The qudit was realized through a set of qubits, and we showed how the proposed mapping can be realized using controlled displacements. A circuit U_v was constructed for the preparation of a qubit state suitable to prepare oscillator GKP states. Our analysis included computing the Wigner function of the oscillator state produced by the protocol with three and four qubits. The results showed a significant improvement in the sharpness of the approximate GKP state with four qubits compared to the three-qubit implementation. This highlights the scalability and effectiveness of our protocol in producing high-quality GKP states with an increasing number of qubits. Finally we investigated the feasibility of the protocol with three qubits, considering various noise sources such as qubit decay, qubit dephasing, oscillator loss, and oscillator dephasing. Overall, our protocol offers a promising approach for efficiently generating highly squeezed GKP states, with robustness against most common noise sources, making it a viable tool for practical quantum computing.

ACKNOWLEDGMENTS

This research is part of the Munich Quantum Valley, which is supported by the Bavarian state government with funds from the Hightech Agenda Bayern Plus. This work is also supported by the Danish National Research Foundation, Center for Macroscopic Quantum States (bigQ, DNRF142). This work is also supported by the European Quantum Flagship Quantum Secure Networks Partnership (EU QSNP) project.

APPENDIX

1. Interpolating function

We evaluate the action of the displacement operator in Eq. (14). We proceed by expanding the Y_N operator in terms of its eigenvectors,

$$\begin{aligned} D_x(s)\sum_{l\in K} v_l|x_l\rangle &= \sum_{l\in K} v_l e^{-i\frac{2\pi}{M}Y_N s}|x_l\rangle \\ &= \sum_{l\in K} v_l \sum_{n\in K} e^{-i\frac{2\pi}{M}ns}|y_n\rangle\langle y_n|x_l\rangle \\ &= \frac{1}{\sqrt{M}}e^{-i\frac{\pi}{M}s}\sum_{l\in K} v_l \\ &\quad\times \sum_{n\in K} e^{i2\pi(n-1/2)(-s-l+1/2)/M}|y_n\rangle \\ &= e^{-i\frac{\pi}{M}s}\sum_{m\in K}\left[\frac{1}{M}\sum_{n,l\in K} v_l e^{i2\pi(n-1/2)(m-s-l)/M}\right] \\ &\quad\times |x_m\rangle \\ &= e^{-i\frac{\pi}{M}s}\sum_{m\in K} v(m-s)|x_m\rangle, \end{aligned} \tag{A1}$$

where

$$v(y) = \frac{1}{M}\sum_{n,l\in K} v_l e^{i2\pi(n-1/2)(y-l)/M}. \tag{A2}$$

By summing the geometric series one can readily verify that $v(k)$ equals v_k for $k\in K$. Furthermore, calculating the Fourier coefficient of $v(y)$ corresponding to the frequency m/M (with $m\in\mathbb{Z}$) over the range R_0, we find

$$\begin{aligned} c_m &= \frac{1}{\sqrt{M}}\int_{-M/2}^{M/2} dy\, v(y)e^{-i2\pi\frac{m}{M}y} \\ &= \frac{1}{M^{3/2}}\sum_{n,l\in K} v_l e^{-i2\pi(n-1/2)l/M}\int_{-M/2}^{M/2} dy\, e^{i2\pi y[n-1/2-m]/M} \\ &= \frac{1}{\sqrt{M}}\sum_{l\in K}\sum_{n=-M/2}^{M/2-1} v_l e^{-i2\pi nl/M}\delta(n-m) \\ &= \begin{cases} \frac{1}{\sqrt{M}}\sum_{l\in K} v_l e^{-i2\pi ml/M} & \text{if } m\in[-M/2;M/2-1], \\ 0 & \text{otherwise,} \end{cases} \end{aligned} \tag{A3}$$

where the δ is a Kronecker δ. So we can write the Fourier coefficient of $v(y)$ associated with frequency m/M as,

$$c_m = \begin{cases} \langle\phi_m|v\rangle & \text{if } m\in[-M/2;M/2-1], \\ 0 & \text{otherwise,} \end{cases} \tag{A4}$$

where we defined the plane wave,

$$|\phi_m\rangle = \frac{1}{\sqrt{M}}\sum_{l\in K} e^{i2\pi ml/M}|x_l\rangle. \tag{A5}$$

It follows, that as long as $\langle\phi_m|v\rangle$ is only large for $|m|\ll M/2$, then the frequencies of $v(y)$ will be significantly below $1/2$. The interpolation $v(y)$ of the points (k, v_k) can then be considered reasonable, in the sense that there will be little oscillatory behavior between the interpolated points (k, v_k).

2. Frame transformations

We assume that the density matrix ρ evolves according to a master equation in Lindblad form,

$$\partial_t\rho = -i[H/\hbar, \rho] + \sum_i \kappa_i D[L_i]\rho \tag{A6}$$

with $D[L_i]\rho = L_i\rho L_i^\dagger - \frac{1}{2}(L_i^\dagger L_i\rho + \rho L_i^\dagger L_i)$ and L_i is the jump operator and κ_i is the jump rate. We make the frame transformation,

$$\tilde{\rho} = U\rho U^\dagger \tag{A7}$$

thereby obtaining the new equation of motion,

$$\partial_t\tilde{\rho} = -i[i\dot{U}U^\dagger + U(H/\hbar)U^\dagger, \tilde{\rho}] + \sum_i \kappa_i D[UL_iU^\dagger]\tilde{\rho}. \tag{A8}$$

3. Hamiltonian

We use the dispersive Hamiltonian with a drive $\varepsilon(t)$,

$$\begin{aligned} H/\hbar &= \sum_{n=1}^{N}\left\{\chi^{(n)}a^\dagger a\frac{\sigma_z^{(n)}}{2} + \frac{1}{2}\omega_q^{(n)}\sigma_z^{(n)}\right\} \\ &\quad + \varepsilon^*(t)a + \varepsilon(t)a^\dagger + \omega_o a^\dagger a, \end{aligned} \tag{A9}$$

where $\sigma_z = |0\rangle\langle 0| - |1\rangle\langle 1|$ and ω_o is the angular frequency of the oscillator. We change to the rotating frame,

$$U_1 = e^{i\omega_o a^\dagger a t + i\frac{1}{2}\sum_{n=1}^{N}\omega_q^{(n)}\sigma_z^{(n)}t}, \tag{A10}$$

thereby obtaining the Hamiltonian,

$$\begin{aligned} H_1/\hbar &= i\dot{U}_1U_1^\dagger + U_1(H/\hbar)U_1^\dagger \\ &= \sum_{n=1}^{N}\frac{1}{2}\chi^{(n)}a^\dagger a\sigma_z^{(n)} + \varepsilon^*(t)e^{-i\omega_o t}a + \varepsilon(t)e^{i\omega_o t}a^\dagger. \end{aligned} \tag{A11}$$

We change to a displaced frame,

$$U_2 = e^{\alpha^*(t)a - \alpha(t)a^\dagger}. \tag{A12}$$

The new Hamiltonian is,

$$\begin{aligned} H_2/\hbar &= i\dot{U}_2U_2^\dagger + U_2(H_1/\hbar)U_2^\dagger \\ &= \sum_{n=1}^{N}\left\{\frac{1}{2}\chi^{(n)}a^\dagger a\sigma_z^{(n)} + \frac{1}{2}\chi^{(n)}|\alpha(t)|^2\sigma_z^{(n)}\right. \\ &\quad \left. + \frac{1}{2}\chi^{(n)}\big(\alpha(t)a^\dagger + \alpha^*(t)a\big)\sigma_z^{(n)}\right\} \\ &\quad + \phi(t)^*a + \phi(t)a^\dagger + \beta(t), \end{aligned} \tag{A13}$$

where

$$\beta(t) = \varepsilon^*(t)e^{-i\omega_o t}\alpha(t) + \varepsilon(t)e^{i\omega_o t}\alpha^*(t), \tag{A14}$$

$$\phi(t) = \varepsilon(t)e^{i\omega_o t} - i\dot{\alpha}(t). \tag{A15}$$

4. Lindbladians

The corresponding transformations of the Lindbladians, resulting from the frame transformations, are,

Oscillator loss.

$$D[U_2U_1aU_1^\dagger U_2^\dagger]\rho = D[a]\rho - \tfrac{1}{2}\alpha(t)[a^\dagger,\rho] + \tfrac{1}{2}\alpha(t)^*[a,\rho]. \tag{A16}$$

Oscillator dephasing.

$$D[U_2U_1a^\dagger aU_1^\dagger U_2^\dagger]\rho = D[(a^\dagger+\alpha(t)^*)(a+\alpha(t))]\rho. \tag{A17}$$

Qubit decay.

$$D[U_2U_1\sigma_-^{(n)}U_1^\dagger U_2^\dagger]\rho = D[\sigma_-^{(n)}]\rho, \tag{A18}$$

where $\sigma_- = |1\rangle\langle 0|$.

Qubit dephasing.

$$D\big[U_2U_1\tfrac{1}{2}\sigma_z^{(n)}U_1^\dagger U_2^\dagger\big]\rho = D\big[\tfrac{1}{2}\sigma_z^{(n)}\big]\rho. \tag{A19}$$

5. Master equation in frame $\mathcal{D}$

Letting $\rho_{\mathcal{D}} = U_2U_1\rho U_1^\dagger U_2^\dagger$, then the master equation in this frame states,

$$\begin{aligned}\partial_t\dot{\rho_{\mathcal{D}}} = &-i\left[H_2/\hbar + \frac{1}{2}i\kappa_l(\alpha(t)^*a-\alpha(t)a^\dagger),\rho_{\mathcal{D}}\right]\\ &+\kappa_l D[a]\rho_{\mathcal{D}} + 2\kappa_\phi D[(a^\dagger+\alpha(t)^*)(a+\alpha(t))]\rho_{\mathcal{D}}\\ &+\sum_{n=1}^{N}\left\{\gamma_l D[\sigma_-^{(n)}]\rho_{\mathcal{D}} + 2\gamma_\phi D\left[\frac{1}{2}\sigma_z^{(n)}\right]\rho_{\mathcal{D}}\right\},\end{aligned} \tag{A20}$$

from which we obtain the effective Hamiltonian,

$$\begin{aligned}H_{\text{eff}}/\hbar &= H_2/\hbar + \frac{1}{2}i\kappa_l(\alpha(t)^*a-\alpha(t)a^\dagger)\\ &= \sum_{n=1}^{N}\left\{\frac{1}{2}\chi^{(n)}a^\dagger a\sigma_z^{(n)} + \frac{1}{2}\chi^{(n)}|\alpha(t)|^2\sigma_z^{(n)}\right.\\ &\quad\left.+\frac{1}{2}\chi^{(n)}(\alpha(t)a^\dagger+\alpha^*(t)a)\sigma_z^{(n)}\right\}\\ &\quad+\left(\phi(t)^*+\frac{1}{2}i\kappa_l\alpha(t)^*\right)a + \left(\phi(t)-\frac{1}{2}i\kappa_l\alpha(t)\right)a^\dagger.\end{aligned} \tag{A21}$$

We then require that the drive $\varepsilon(t)$ (approximately) satisfy the following equation,

$$\phi(t) - \tfrac{1}{2}i\kappa_l\alpha(t) = \varepsilon(t)e^{i\omega_o t} - i\dot{\alpha}(t) - \tfrac{1}{2}i\kappa_l\alpha(t) = 0. \tag{A22}$$

The effective Hamiltonian is then,

$$\begin{aligned}H_{\text{eff}}/\hbar = \sum_{n=1}^{N}&\left\{\frac{1}{2}\chi^{(n)}a^\dagger a\sigma_z^{(n)} + \frac{1}{2}\chi^{(n)}|\alpha(t)|^2\sigma_z^{(n)}\right.\\ &\left.+\frac{1}{2}\chi^{(n)}\big(\alpha(t)a^\dagger+\alpha^*(t)a\big)\sigma_z^{(n)}\right\}.\end{aligned} \tag{A23}$$

[1] D. Gottesman, A. Kitaev, and J. Preskill, Encoding a qubit in an oscillator, Phys. Rev. A **64**, 012310 (2001).

[2] A. L. Grimsmo and S. Puri, Quantum error correction with the Gottesman-Kitaev-Preskill code, Phys. Rev. X Quantum **2**, 020101 (2021).

[3] B. W. Walshe, B. Q. Baragiola, R. N. Alexander, and N. C. Menicucci, Continuous-variable gate teleportation and bosonic-code error correction, Phys. Rev. A **102**, 062411 (2020).

[4] J. E. Bourassa, R. N. Alexander, M. Vasmer, A. Patil, I. Tzitrin, T. Matsuura, D. Su, B. Q. Baragiola, S. Guha, G. Dauphinais, K. K. Sabapathy, N. C. Menicucci, and I. Dhand, Blueprint for a scalable photonic fault-tolerant quantum computer, Quantum **5**, 392 (2021).

[5] B. Q. Baragiola, G. Pantaleoni, R. N. Alexander, A. Karanjai, and N. C. Menicucci, All-Gaussian universality and fault tolerance with the Gottesman-Kitaev-Preskill code, Phys. Rev. Lett. **123**, 200502 (2019).

[6] S. Muralidharan, L. Li, J. Kim, N. Lütkenhaus, M. D. Lukin, and L. Jiang, Optimal architectures for long distance quantum communication, Sci. Rep. **6**, 20463 (2016).

[7] K. Fukui, R. N. Alexander, and P. van Loock, All-optical long-distance quantum communication with Gottesman-Kitaev-Preskill qubits, Phys. Rev. Res. **3**, 033118 (2021).

[8] P. Dhara, L. Jiang, and S. Guha, Entangling quantum memories at channel capacity, arXiv:2406.04272.

[9] P. Dhara, L. Jiang, and S. Guha, Interfacing Gottesman-Kitaev-Preskill qubits to quantum memories, arXiv:2406.04275 [Phys. Rev. A (to be published)].

[10] X. C. Kolesnikow, R. W. Bomantara, A. C. Doherty, and A. L. Grimsmo, Gottesman-Kitaev-Preskill state preparation using periodic driving, Phys. Rev. Lett. **132**, 130605 (2024).

[11] J. Hastrup, K. Park, J. Brask, R. Filip, and U. Andersen, Measurement-free preparation of grid states, npj Quantum Inf. **7**, 17 (2021).

[12] J. Hastrup and U. L. Andersen, Protocol for generating optical Gottesman-Kitaev-Preskill states with cavity QED, Phys. Rev. Lett. **128**, 170503 (2022).

[13] S. Konno, W. Asavanant, F. Hanamura, H. Nagayoshi, K. Fukui, A. Sakaguchi, R. Ide, F. China, M. Yabuno, S. Miki, H. Terai, K. Takase, M. Endo, P. Marek, R. Filip, P. van Loock, and A. Furusawa, Logical states for fault-tolerant quantum computation with propagating light, Science **383**, 289 (2024).

[14] D. J. Weigand and B. M. Terhal, Generating grid states from Schrödinger-cat states without postselection, Phys. Rev. A **97**, 022341 (2018).

[15] I. Tzitrin, J. E. Bourassa, N. C. Menicucci, and K. K. Sabapathy, Progress towards practical qubit computation using approximate Gottesman-Kitaev-Preskill codes, Phys. Rev. A **101**, 032315 (2020).

[16] K. Takase, K. Fukui, A. Kawasaki, W. Asavanant, M. Endo, J. ichi Yoshikawa, P. van Loock, and A. Furusawa, Gottesman-Kitaev-Preskill qubit synthesizer for propagating light, npj Quantum Inf. **9**, 98 (2023).

[17] B. M. Terhal and D. Weigand, Encoding a qubit into a cavity mode in circuit QED using phase estimation, Phys. Rev. A **93**, 012315 (2016).

[18] Y. Shi, C. Chamberland, and A. Cross, Fault-tolerant preparation of approximate GKP states, New J. Phys. **21**, 093007 (2019).

[19] K. R. Motes, B. Q. Baragiola, A. Gilchrist, and N. C. Menicucci, Encoding qubits into oscillators with atomic ensembles and squeezed light, Phys. Rev. A **95**, 053819 (2017).

[20] R. Dahan, G. Baranes, A. Gorlach, R. Ruimy, N. Rivera, and I. Kaminer, Creation of optical cat and GKP states using shaped free electrons, Phys. Rev. X **13**, 031001 (2023).

[21] C. Flühmann, T. L. Nguyen, M. Marinelli, V. Negnevitsky, K. Mehta, and J. P. Home, Encoding a qubit in a trapped-ion mechanical oscillator, Nature (London) **566**, 513 (2019).

[22] B. de Neeve, T.-L. Nguyen, T. Behrle, and J. P. Home, Error correction of a logical grid state qubit by dissipative pumping, Nat. Phys. **18**, 296 (2022).

[23] P. Campagne-Ibarcq, A. Eickbusch, S. Touzard, E. Zalys-Geller, N. E. Frattini, V. V. Sivak, P. Reinhold, S. Purl, S. Shankar, R. J. Schoelkopf, L. Frunzio, M. Mirrahimi, and M. H. Devoret, Quantum error correction of a qubit encoded in grid states of an oscillator, Nature (London) **584**, 368 (2020).

[24] A. Eickbusch, V. Sivak, A. Z. Ding, S. S. Elder, S. R. Jha, J. Venkatraman, B. Royer, S. M. Girvin, R. J. Schoelkopf, and M. H. Devoret, Fast universal control of an oscillator with weak dispersive coupling to a qubit, Nat. Phys. **18**, 1464 (2022).

[25] Y. Aharonov and D. Rohrlich, *Quantum Paradoxes* (Wiley, New York, 2005).

[26] B. C. Travaglione and G. J. Milburn, Preparing encoded states in an oscillator, Phys. Rev. A **66**, 052322 (2002).

[27] M. Nielsen and I. Chuang, *Quantum Computation and Quantum Information* (Cambridge University Press, Cambridge, 2010).

[28] T. S. Santhanam and A. R. Tekumalla, Quantum mechanics in finite dimensions, Found. Phys. **6**, 583 (1976).

[29] A. Blais, A. L. Grimsmo, S. M. Girvin, and A. Wallraff, Circuit quantum electrodynamics, Rev. Mod. Phys. **93**, 025005 (2021).

[30] G. S. Agarwal, *Quantum Optics* (Cambridge University Press, Cambridge, 2013).